Received: 2 November 2016 | Accepted: 18 January 2017
DOI: 10.1002/chir.22680

REGULAR ARTICLE

WILEY

Chiral exploration of 6,12-diphenyldibenzo[*b*,*f*][1,5]diazocine with stable conformation

Zheng-Yi Li | **Yong Pan** | **Lin-Lin Jin** | **Yue Yin** | **Bao-Zhu Yang** | **Xiao-Qiang Sun**

Jiangsu Key Laboratory of Advanced Catalytic Materials and Technology, School of Petrochemical Engineering, Changzhou University, Changzhou, P.R. China

Correspondence
Zheng-Yi Li, Jiangsu Key Laboratory of Advanced Catalytic Materials and Technology, School of Petrochemical Engineering, Changzhou University, Changzhou 213164, P.R. China.
Email: zyli@cczu.edu.cn; sunxiaoqiang@yahoo.com

Funding Information
NSFC, Grant/Award Number: 21572026 and 21002009; Natural Science Foundation of Jiangsu Colleges and Universities, Grant/Award Number: 14KJA150002; Advanced Catalysis and Green Manufacturing Collaborative Innovation Center, Grant/Award Number: ACGM2016-06-05; Priority Academic Program Development of Jiangsu Higher Education Institutions

Abstract

A first optical resolution of 6,12-diphenyldibenzo[*b*,*f*][1,5]diazocine with stable boat conformation was achieved by chiral supercritical fluid chromatography (SFC). The absolute configurations of enantiomers were first assigned and determined by X-ray crystal structure based on CIP-rules. The high optical rotation and circular dichroism spectrum were well explained by electronic helix theory. Owing to the high stabilization of boat conformation, the chiral configuration could be maintained at very high temperature, more than 200 °C, which was proved by Density Functional Theory calculations.

KEYWORDS
chirality, diazocine, high optical rotation, optical resolution, stable conformation

1 | INTRODUCTION

Chirality plays a pivotal role in chemistry, medicine, biochemistry, and materials science.[1-6] Classic chirality based on sp^2 hybridized stereogenic centers has been well investigated, while less emphasis has been devoted to inherent chirality induced only by special molecular conformation. Recently, the concept of conformational chirality based on axial and planar chiral molecules has become a topic of intense interest.[7-15] Different kinds of structures with the restricted rotation of σ-bonds such as biaryls, cyclophanes, and strained cyclic alkenes have been developed for asymmetric catalysis, functional materials, supramolecular chemistry, targets of total synthesis, and so on.[16-20]

Increasing the conformational stability gives higher chances for optical resolution of conformationally chiral molecules. As shown in Scheme 1, it is well known that dibenzo[*a*,*e*]cyclooctene **1** with a flexible conformations of boat-to-boat interconversion shows many interesting photoelectric activities.[21] When the two $C=C$ bonds are exchanged for (thio)amide units to form di(thio)anthranilides **2**, the conformational interconversion becomes hindered. This allowed one to optically resolve these chiral compounds.[22,23] Herein, we thought that 6,12-diphenyldibenzo[*b*,*f*][1,5]diazocine **3** may possess a more stable chiral conformation because of the rigidity of $C=N$ bonds.

Since the skeleton of benzo[*b*,*f*][1,5]diazocine was first synthesized more than century ago,[24] substantial efforts have been devoted to the preparation and application of the racemic mixtures.[25-36] However, to the best of our knowledge, the chirality of this type of compound has not been investigated yet. Herein, we report the successful optical resolution of **3** and experimental determination of absolute configurations of its enantiomers and the properties directly connected to their chirality.

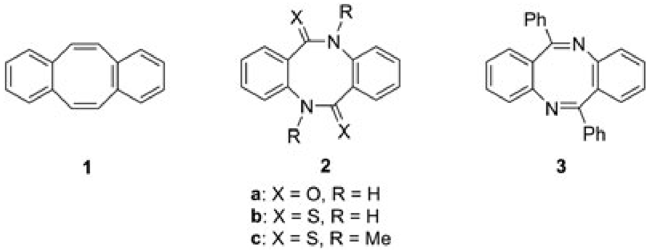

SCHEME 1 Structures of dibenzo[*a*,*e*][8]annulene **1**, di(thio) anthralinides **2** and 6,12-diphenyldibenzo[*b*,*f*] [1,5]diazocine **3**

2 | MATERIALS AND METHODS

All reactions were performed under an atmosphere of air unless noted otherwise. The commercially available reagents and solvents were used without further purification unless otherwise noted. Nuclear magnetic resonance (NMR) spectra were recorded on a Bruker (Billerica, MA) AVANCE III 300 MHz NMR spectrometer equipped with a 5 mm BBO probe. The analytic and preparative chiral supercritical fluid chromatography (SFC) were carried out on MD-2018 Plus and Novasep-3050 instruments, respectively. Optical rotations were measured using an automatic polarimeter of Rudolph-IV. Single crystal X-ray diffraction was conducted on a Bruker APEX-II X-ray diffractometer equipped with a CCD area director. Melting points (without correction) were measured using an SGW X-4 micro-melting point apparatus. The UV–Vis and CD spectra were measured on Shimazhu UV-1700 and JASCO-810, respectively.

2.1 | 6,12-diphenyldibenzo[*b*,*f*][1,5]diazocine (3)[25]

A mixture of 2-aminobenzophenone (7.88 g, 40 mmol) and phosphorus pentaoxide (1.14 g, 8 mmol) was stirred at 120 °C without any solvent. The reaction mixture was kept at this temperature for 5 h until the reaction was completed (monitored by thin-layer chromatography [TLC]). The reaction mixture was treated with water (20 mL) and then extracted with dichloromethane (3 × 30 mL). The organic layer was washed with brine and dried over anhydrous Na_2SO_4. The dichloromethane was evaporated under vacuum, and the residue was recrystallized from n-hexane/dichloromethane (v:v = 5:1) to afford light yellow crystals in 85% yield. Mp: 185–187 °C (Lit.[37] 191–193 °C). ^{1}H NMR (300 MHz, $CDCl_3$) δ (ppm): 7.78–7.75 (m, 4H), 7.40–7.25 (m, 8H), 7.05–6.95 (m, 6H). ^{13}C NMR (75 MHz, $CDCl_3$) δ (ppm): 169.6, 159.9, 138.0, 131.1, 129.7, 129.4, 128.2, 127.6, 126.9, 123.4, 120.9. ESI-MS: $m/z = 359\ [M + H]^+$.

3 | RESULTS AND DISCUSSION

The racemic (±)-**3** was prepared by the self-condensation of 2-aminobenzophenone in the presence of P_2O_5 under solvent-free conditions.[25-36] The X-ray crystal structure of racemic (±)-**3**[38] revealed that there are two enantiomers with opposite configurations (*R* vs. *S*) in the unite cell (Figure 1a). Both of

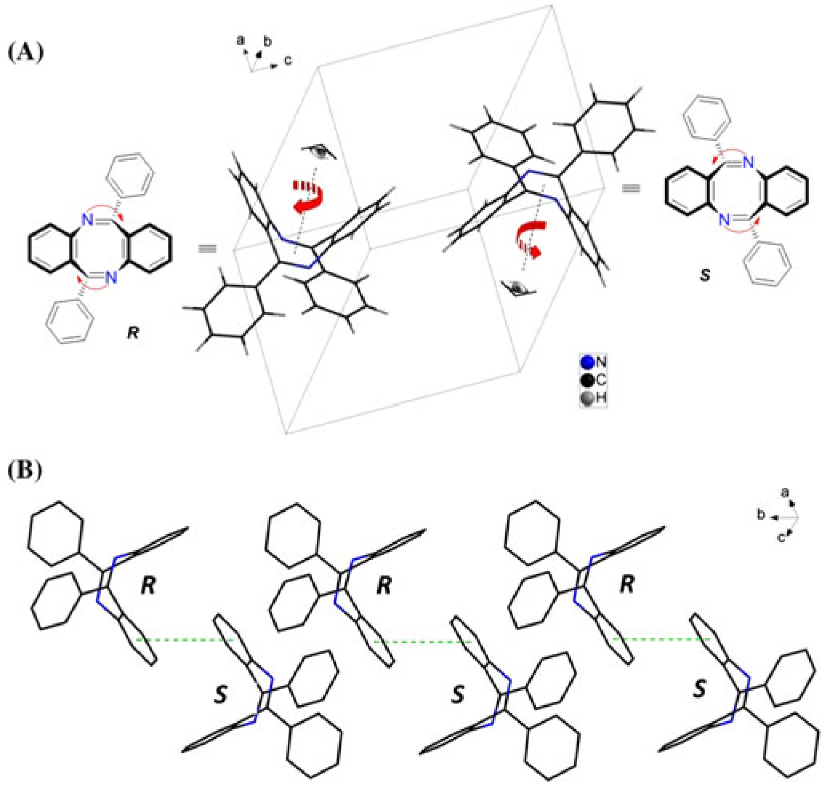

FIGURE 1 **A**, The X-ray crystal structure of racemic (±)-**3** in the unit cell and assignment of absolute configuration. **B**, Packing of racemic (±)-3 along the *b* axis. The hydrogen atoms are omitted for clarity

the two molecules adopt the boat conformation similar to a "saddle," where the dibenzo[*b*,*f*][1,5]diazocine parent skeleton looks like a horse blanket with two handles, while the other two phenyl groups look like a pair of stirrups. To assign the chiral configuration, we propose the method based on the Cahn-Ingold-Prelog (CIP) rule.[39-42] As depicted in Figure 1a, first, two C = N bonds were placed in the plane of the figure. Then two benzenes annelated with an eight-membered ring should be located in front of the figure, while the two phenyl substituents should be placed behind as the group(s) with the lowest priority. Finally, according to the priority of atoms (groups), the directionality within the eight-membered ring should be counted from nitrogen to the doubly bonded carbon atom. In other words, from N to C within N = C bond. Therefore, the absolute configuration of **3** can be assigned as *R* in the case of clockwise or *S* in the case of counterclockwise directionality.

To further survey the relationship between the structure and chirality, the racemic (±)-**3** was resolved by chiral SFC, and the two fractions (**I** and **II**) corresponding to the two enantiomers of **3** were obtained in high optical purity (>99% *ee*), respectively (Supporting Information, Figure S1). According to the rule proposed above (Figure 1a), the X-ray crystal structure of **II-3**[38] revealed that the molecule adopts *R* configuration (Figure 2). So, the configuration of the first fraction **I-3** must be *S* (the inverse one). Moreover, different molecular packing modes between chiral molecule **II**-**3** and racemic (±)-**3** are observed. Intermolecular C–H···N and π–π weak interactions link the molecules in *R*-configuration to form a chiral zig-zag chain along *b* axis in **II-3** (Figure 3 and Table 1), while only weak intermolecular π–π interactions between the two opposite enantiomers lead to the formation of overall achiral dimers as independent units of racemic (±)-**3** (Figure 1b and Table 1).

Optical rotation of the two fractions were then measured, and the results showed that they possess quite large rotation angles of −1916° for **I-3** and +1923° for **II-3** ($[\alpha]_D^{25}$, *c* = 1, CH_2Cl_2). Such high optical rotation can be ascribed to the highly twisted (the dihedral angle between phenyl rings A and B in X-ray crystal structure of **II-3** is 85.2°, Figure 2) and stable boat conformation of the eight-member ring. According to the electronic helix theory,[43-48] an electron is constrained to move on a helix, which leads to optical rotation of polarized light. The capability of this rotation can be extremely influenced by electronic polarizability. The greater the electronic polarizability, the greater the rotation of the helix. Furthermore, more turns of helices with conjugate system also can conduct high optical rotation.[49] The structure of **II-3** can be seen as the one having two turns of helices (Figure 4). The first one is induced by the two C = C aromatic bonds of two benzenes annelated with an eight-membered ring of the bis-imine system. The second one involves two C = N imine bonds and is additionally induced by the different electronegativity of the N and C atoms, which can drastically enhance the rotation of polarized light.

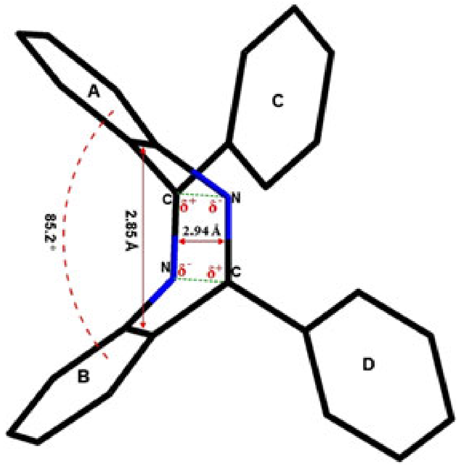

FIGURE 2 The X-ray crystal structure of **II-3**. The hydrogen atoms are omitted for clarity

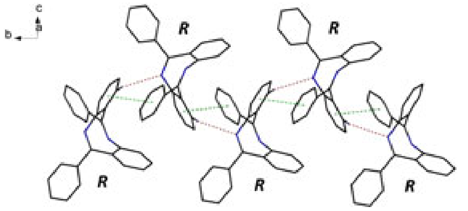

FIGURE 3 Packing of chiral **II**-(+)-**3** along the *b* axis. The hydrogen atoms except those involved in hydrogen bonding are omitted for clarity

Subsequently, the circular dichroism (CD) spectra of the two enantiomers **I**-(−)-*S*-**3** and **II**-(+)-*R*-**3** were studied in detail. The two CD curves are perfect mirror images of each other, reflecting the opposite configuration of the inherently chiral skeletons (Figure 5). Based on the electronic helix theory,[43-48] the imine group conjugated with an aryl ring constitutes a chromophore, the helicity of which determines the Cotton effect sign. For **II**-(+)-*R*-**3**, combined with UV–Vis spectrum (Supporting Information, Figure S2), the positive long wavelength Cotton effect at 328 nm is due to the n–π^* transition and reflects the helicity of the twisted phenylmethanimine chromophore. According to the X-ray structure of **II**-(+)-*R*-**3** (Figure 2). it is twisted in the *P* sense (the two N = C–C = C torsion angles of the eight-membered ring are 64.7(2)° and 69.3(3)°, respectively). It is a close analogy to α,β-unsaturated carbonyl systems[50-52] and di(thio) anthranilides **2**,[22,23] where the *P*-helicity of the chromophore leads to the positive n–π^* Cotton effect sign, whereas the *M*-helicity causes the negative one. The other negative Cotton effects at 263 nm can be attributed to the π–π^* transition. The electric transition moment was 2.514 D, which was calculated by time-dependent Density Functional Theory (TDDFT) at the B3LYP/6-31G* level with the Gaussian09 software package.[53] Owing to the polarizability sequences

TABLE 1 Intermolecular weak interactions of **II**-(+)-**3** and (±)-**3** along *b* axis

Compound	D–H...A (π...π)	d (D–H)	d (H...A)	d (D...A) d (Centroid...Centroid)	∠DHA (Dihedral angle)	ST
II-(+)-**3**	C(19)–H(19)...N(1)	0.93	2.76	3.32	119.94	2-x, −1/2 + y,1/2-z
	Cg(1)[a]...Cg(2)[b]	—	—	3.94	8.27	2-x, −1/2 + y,1/2-z
(±)-**3**	Cg(3)...Cg(3)[c]	—	—	4.15	0	2-x,1-y,-z

D: donor atom; A: acceptor atom; ST: symmetry transformation for the acceptor atom.

[a] Cg(1) is the centroid of the phenyl ring C(19)-C(24) of **II**.

[b] Cg(2) is the centroid of the phenyl ring C(1)-C(6) of **II**.

[c] Cg(3) is the centroid of the phenyl ring C(7)-C(12) of (±)-**3**.

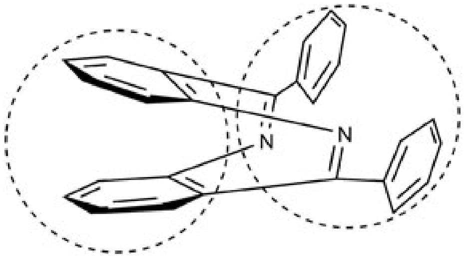

FIGURE 4 The molecular structure of **II**-(+)-**3** with two polarized π-electronic helixes

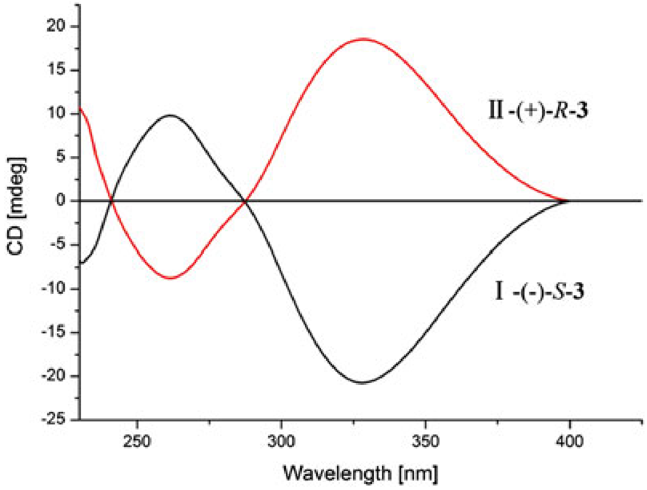

FIGURE 5 CD spectra of **I**-(−)-*S*-**3** and **II**-(+)-*R*-**3** in CH_2Cl_2 at 25 °C

FIGURE 6 The geometry of **II**-(+)-*R*-**3** and the polarized diction of π electron

of N > C, the geometry of **II**-(+)-*R*-**3** implies the left-handed screwness (counterclockwise orientation) of the π–π* transition moments, in agreement with the observed negative CD signal[22,23,43-48,50-52] (Figures 5, 6). F6

Finally, the conformational (chiral) stability of **3** was investigated. The two optically pure enantiomers **I**-(−)-*S*-**3** and **II**-(+)-*R*-**3** were heated separately at 200 °C (melt state) for 5 h, and the results demonstrated that the chiral conformation of **3** can be preserved even at this high temperature (Supporting Information, Figure S3). This might be ascribed to two reasons (Figure 2). 1) in the eight-member ring, there are still some weak π–π interactions between the two pairs of parallel C = N (distance: 2.94 Å) and C = C (distance: 2.85 Å), which both can enhance the conformational stability; 2) in the two C = N bonds, C atoms have partial positive while N atoms bear partial negative charges, which lead to electrostatic attraction between the two C = N bonds. As a result, the molecular structure of **3** possesses very stable conformation to retain chirality. The energy barrier of conformational inversion was also calculated (Figure 7). The ground state (boat conformation with *R* or *S* configuration) and transition state (planar conformation) structures of **3** were optimized by DFT at the B3LYP/6-31G* level with the Gaussian09 software package.[53] The calculation results showed that the energy barrier to ring inversion was

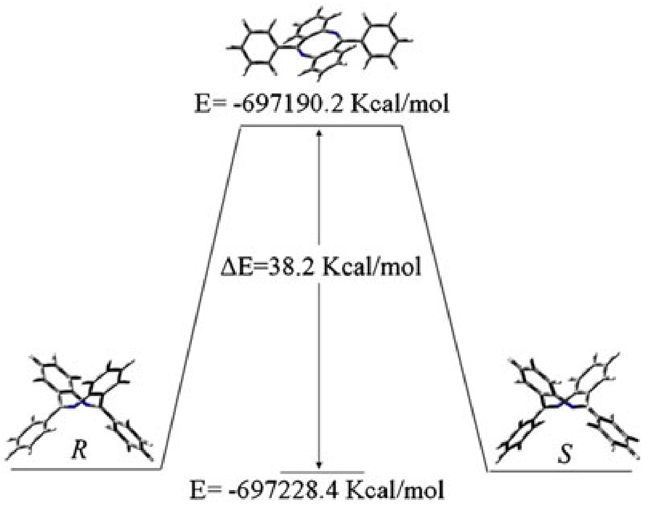

FIGURE 7 Relative energy diagram of the boat-to-boat inversion of **3** from *R* to *S* configuration calculated by DFT

38.2 kcal/mol, which further proved that the boat conformation of **3** was very stable.

4 | CONCLUSION

In conclusion, we have successfully resolved 6,12-diphenylbenzo[*b*,*f*][1,5]diazocine **3** by chiral supercritical fluid chromatography for the first time. The chirality of **3** is induced by the nonplanarity of the diaza-eight-membered ring and the fixed directionality within it. The absolute configurations of the two optically pure enantiomers were assigned and determined by analogous CIP rules and crystal X-ray diffraction, respectively. The very high conformational inversion barrier makes it possible to retain the chirality completely even after prolonged heating at 200 °C in the melt state. Their high optical rotation and CD spectrum are well explained by electronic helix theory.

ACKNOWLEDGEMENTS

This work is supported by NSFC (Nos. 21572026 and 21002009), the Natural Science Foundation of Jiangsu Colleges and Universities (14KJA150002), Advanced Catalysis and Green Manufacturing Collaborative Innovation Center, Changzhou University (ACGM2016-06-05), and the Priority Academic Program Development of Jiangsu Higher Education Institutions.

REFERENCES

1. Moll PJW, Nair NL, Helm T, et al. Transport evidence for Fermi-arc-mediated chirality transfer in the Dirac semimetal Cd_3As_2. *Nature*. 2016;535:266-270.
2. Lundeberg MB, Folk JA. Harnessing chirality for valleytronics. *Science*. 2014;346:422-423.
3. Tee YH, Shemesh T, Thiagarajan V, et al. Cellular chirality arising from the self-organization of the actin cytoskeleton. *Nature*. 2015;17:445-457.
4. Gu ZG, Zhan CH, Zhang J, Bu XH. Chiral chemistry of metal-camphorate frameworks. *Chem Soc Rev*. 2016;45:3122-3144.
5. Shen J, Okamoto Y. Efficient separation of enantiomers using stereoregular chiral polymers. *Chem Rev*. 2016;116:1094-1138.
6. Sunoj RB. Transition state models for understanding the origin of chiral induction in asymmetric catalysis. *Acc Chem Res*. 2016;49:1019-1028.
7. Reen M, O'Sullivan TP. The application of molecular tethers in controlling axial chirality. *Mini-Rev Org Chem*. 2016;13:206-218.
8. Zheng J, Cui WJ, Zheng C, You SL. Synthesis and application of chiral spiro Cp ligands in rhodium-catalyzed asymmetric oxidative coupling of biaryl compounds with alkenes. *J Am Chem Soc*. 2016;138:5242-5245.
9. Ishida N, Sawano S, Murakami M. Stereospecific ring expansion from orthocyclophanes with central chirality to metacyclophanes with planar chirality. *Nat Commun*. 2014;5:3111-3111.
10. Yoshioka S, Inokuma Y, Hoshino M, Sato T, Fujita M. Absolute structure determination of compounds with axial and planar chirality using the crystalline sponge method. *Chem Sci*. 2015;6:3765-3768.
11. Barrett KT, Metrano AJ, Rablen PR, Miller SJ. Spontaneous transfer of chirality in an atropisomerically enriched two-axis system. *Nature*. 2014;509:71-75.
12. Di Iorio N, Righi P, Mazzanti A, Mancinelli M, Ciogli A, Bencivenni G. Remote control of axial chirality: Aminocatalytic desymmetrization of N-arylmaleimides via vinylogous michael addition. *J Am Chem Soc*. 2014;136:10250-10253.
13. Zheng ZG, Li YN, Bisoyi HK, Wang L, Bunning TJ, Li Q. Three-dimensional control of the helical axis of a chiral nematic liquid crystal by light. *Nature*. 2016;531:352-356.
14. Campolo D, Gastaldi S, Roussel C, Bertrand MP, Nechab M. Axial-to-central chirality transfer in cyclization processes. *Chem Soc Rev*. 2013;42:8434-8466.
15. Yang L, Zheng HY, Luo L, et al. Palladium-catalyzed dynamic kinetic asymmetric transformation of racemic biaryls: Axial-to-central chirality transfer. *J Am Chem Soc*. 2015;137:4876-4879.
16. Bringmann G, Gulder T, Gulder TAM, Breuning M. Atroposelective total synthesis of axially chiral biaryl natural products. *Chem Rev*. 2011;111:563-639.
17. Bisoyi HK, Li Q. Light-directing chiral liquid crystal nanostructures: From 1D to 3D. *Acc Chem Res*. 2014;47:3184-3195.
18. Zhang X, Yin J, Yoon J. Recent advances in development of chiral fluorescent and colorimetric sensors. *Chem Rev*. 2014;114:4918-4959.
19. Brandt JR, Wang X, Yang Y, Campbell AJ, Fuchter MJ. Circularly polarized phosphorescent electroluminescence with a high dissymmetry factor from PHOLEDs based on a platinahelicene. *J Am Chem Soc*. 2016;138:9743-9746.
20. Li L, Liu Y, Peng Y, Yu L, Wu X, Yan H. Kinetic resolution of β-sulfonyl ketones through enantioselective β-elimination using a cation-binding polyether catalyst. *Angew Chem Int Ed*. 2016;55:331-335.
21. Yuan C, Saito S, Camacho C, Irle S, Hisaki I, Yamaguchi S. A π-conjugated system with flexibility and rigidity that shows environment-dependent RGB luminescence. *J Am Chem Soc*. 2013;135:8842-8845.
22. Olszewska T, Gdaniec M, Połoński T. Planar chiral dianthranilide and dithiodianthranilide molecules: Optical resolution, chiroptical spectra, and molecular self-assembly. *J Org Chem*. 2004;69:1248-1255.
23. Olszewska T, Gdaniec M, Połoński T. Enantiomeric resolution of N, N-dimethyldithiodianthranilide through diastereomeric silver(I) complex. circular dichroism spectra, racemization barrier, and molecular self-assembly. *J Org Chem*. 2008;73:4859-4864.
24. Sondheimer A. Zur kenntniss eines körpers mit achtgliedrigem ringe. *Chem Ber*. 1896;29:1272-1275.
25. Tanmoy C, Rajiv VK, Maya SS. $InCl_3$-driven regioselective synthesis of functionalized/annulated quinolines: Scope and limitations. *Chem Asian J*. 2012;7:778-787.

26. Pettersson B, Bergman J, Svensson PH. Synthetic studies towards 1,5-benzodiazocines. *Tetrahedron*. 2013;69:2647-2654.
27. Eisch JJ, Yu K, Rheingold AL. 6,12-Diphenyldibenzo[*b,f*][1,5] diazocine as an electron-capture agent: Efficient mechanistic probe for SET processes and reagent for the oxidative dimerization of benzylic organometallics. *Eur J Org Chem*. 2012;3165-3171.
28. Zhao N, Qiu L, Wang X, Li JZ, Jiang Y, Wan XB. Trifluoroacetic acid catalyzed dibenzodiazocine synthesis: Optimization and mechanism study. *Tetrahedron*. 2012;68:9665-9671.
29. Acharya BP, Rao YR. Synthesis of unsymmetrical substituted 6,12-diaryldibenzo[*b*,*f*][1,5]diazocines and their precursor Schiff bases. *Synthesis*. 1986;324-326.
30. Jung DI, Song JH, Lee EJ, Kim YY, Lee DHYG, Hahn JT. Simple synthesis of quinolines and dibenzo[*b*,*f*][1,5]diazocines under microwave irradiation. *Tetrahedron Lett*. 2009;50:5805-5807.
31. Marsella JM. Classic annulenes, nonclassical applications. *Acc Chem Res*. 2002;35:944-951.
32. Suga T, Wi S, Long TE. Synthesis of diazocine-containing poly (arylene ether sulfone)s for tailored mechanical and electrochemical performance. *Macromolecules*. 2009;42:1526-1532.
33. Acharya BP, Misra BK, Rao YR. Mass spectral and pyrolytic studies of some 4,4-disubstituted 1,4-dihydro-2H-3,1-benzoxazin-2-ones. *Bull Chem Soc Jpn*. 1987;60:4417-4420.
34. Metlesicsr W, Tavares R, Sternbach LH. The reduction products of a dibenzo[b,fl[l,5]diazocine*J Org Chem*. 1966;31:3356-3362.
35. Boruah RC, Sandhu JS. A facile synthesis of 2,4,8,10-tetrahalo-6,12-diaryldibenzo[*b*,*f*][1,5]diazocines. *J Heterocycl Chem*. 1988;25:459-462.
36. Duncan GW, Lyster SC, Wright JB. Reproduotive mechanisms influenced by a diazocine. *Proc Soc Exp Biol Med*. 1965;120:725-728.
37. Metlesics W, Resnick T, Silverman G, Tavares R, Sternbach LH. 6, 12-Diphenyldibenzo[*b*,*f*][1,5]diazocines. *J Med Chem*. 1966;9: 633-634.
38. CCDC 946617 (racemic (±)-**3**) and CCDC 930088 (chiral **II-(+)-3**) contains the supplementary crystallographic data for this paper. These data can be obtained free of charge from The Cambridge Crystallographic Data Centre via www.ccdc.cam.ac.uk/data_request/cif.
39. Fujita S. Chirality and stereogenicity for allene derivatives. Observance and violation of chirality fittingness. *Bull Chem Soc Jpn*. 2002;75:19491962.
40. Fujita S. Stereogenicity/astereogenicity as global/local permutation-group symmetry and relevant concepts for restructuring stereochemistry. *J Math Chem*. 2003;33:113-143.
41. Curtis NF. Configurational isomerism of 2,5,5,7,9,12,12,14-octamethyl-1,4,8,11-tetraazacyclotetradecane and its compounds. *Coord Chem Rev*. 2012;256:878-895.
42. Fowler PW, Rassat A. A classification scheme for chiral tetrahedral. *C R Chimie*. 2006;9:1203-1208.
43. Wang DZ. A helix theory for molecular chirality and chiral interaction. *Mendeleev Commun*. 2004;6:244-247.
44. Wang DZ. Conservation of helical asymmetry in chiral interactions. *Tetrahedron*. 2005;61:7125-7133.
45. Wang DZ. Catalyst-substrate helical character matching determines enantiomeric excess. *Tetrahedron*. 2005;61:7134-7143.
46. Wang DZ. Conservation of helicity and helical character matching in chiral interactions. *Chirality*. 2005;17:S177-S182.
47. Han P, Wang RJ, Wang DZ. Electronic polarizability-based stereochemical model for Sharpless AD reactions. *Tetrahedron*. 2011;67:8873-8878.
48. Xing X, Zhao Y, Xu C, Zhao X, Wang DZ. Electronic helix theory-guided rational design of kinetic resolutions by means of the Sharpless asymmetric dihydroxylation reactions. *Tetrahedron*. 2012;68:7288-7294.
49. Meurer KP, Voegtle F. Helical molecules in organic chemistry. *Top Curr Chem*. 1985;127:1-76.
50. Gdaniec M, Połoński T. Generation of chirality in guest aromatic ketones included in the crystals of steroidal bile acids. *J Am Chem Soc*. 1998;120:7353-7354.
51. Jackman LM, Webb RL, Yick HC. Synthesis and chiroptical properties of some piperidin-2-ones. *J Org Chem*. 1982;47:1824-1831.
52. Klyne W, Kirk D, Tilley NJ, Suginome H. Chiroptical studies-part 99: The circular dichroism of seven-membered lactams and lactones. *Tetrahedron*. 1980;36:543-553.
53. The TDDFT and DFT calculations were performed with the Gaussian09 program (see the Supporting Information).

SUPPORTING INFORMATION

Additional Supporting Information may be found online in the supporting information tab for this article.

How to cite this article: Li Z-Y, Pan Y, Jin L-L, Yin Y, Yang B-Z, Sun X-Q. Chiral exploration of 6,12-diphenyldibenzo[*b*,*f*][1,5]diazocine with stable conformation. *Chirality*. 2017;0:00–00. https://doi.org/10.1002/chir.22680